Journal of Advanced Transportation, Vol. 39, No. 3, pp. 323-349
www.advanced-transport.com

Inhomogeneous Cellular Automata Modeling for Mixed Traffic with Cars and Motorcycles

Lawrence W. Lan
Chiung-Wen Chang

This paper develops inhomogeneous cellular automata models to elucidate the interacting movements of cars and motorcycles in mixed traffic contexts. The car and motorcycle are represented by non-identical particle sizes that respectively occupy 6×2 and 2×1 cell units, each of which is 1.25×1.25 meters. Based on the field survey, we establish deterministic cellular automata (CA) rules to govern the particle movements in a two-dimensional space. The instantaneous positions and speeds for all particles are updated in parallel per second accordingly. The deterministic CA models have been validated by another set of field observed data. To account for the deviations of particles' maximum speeds, we further modify the models with stochastic CA rules. The relationships between flow, cell occupancy (a proxy of density) and speed under different traffic mixtures and road (lane) widths are then elaborated.

Keywords: car, inhomogeneous cellular automata, mixed traffic, motorcycle

1. Introduction

Conventional traffic flow models are generally divided into two branches: macroscopic and microscopic models. The macroscopic traffic stream models, single-regime or multiple-regime, are mostly devoted to elucidating the relations between speed, density and flow in various traffic conditions (e.g., free flow, capacity flow, jammed flow) and roadway environments (e.g., tunnel, freeway, urban arterial) [May, 1990]. The macroscopic fluid-dynamical models analogize vehicular flows to

Lawrence W. Lan, Professor, Institute of Traffic and Transportation, National Chiao Tung University, Taiwan
Chiung-Wen Chang, Research Specialist, Institute of Transportation, Ministry of Transportation and Communications, Taiwan
Received: August 2004; Accepted: December 2004

fluids by assuming the aggregate homogeneous behavior of drivers. Lighthill and Whitham [1955] and Richards [1956] developed the most well-known first-order fluid-dynamical models and other researchers such as Payne [1971], Liu, et al. [1998] and Zhang [1998] derived similar but higher order models. Wong and Wong [2002] formulated a multi-class traffic flow model as an extension of LWR model with heterogeneous drivers. Daganzo [1994] developed cell transmission model in which the highway is partitioned into small cells and vehicles move in and out of these cells over time. Daganzo [2002a, 2002b] further proposed a macroscopic behavioral theory to explain the traffic dynamics in homogeneous multi-lane freeways. The microscopic traffic flow models, on the other hand, describe the interrelationship of individual vehicle movements with other vehicles. Car-following models are the most pertinent ones to explicate the one-dimensional movements in a longitudinal lane such that the following vehicle adjusts its speed to maintain desirable or safe spacing (distance headway) with the lead vehicle. The types of car-following models are in general divided into four categories: stimulus-response [e.g., Herman, et al. 1959; Bierley, 1963; Pipes, 1967; Rockwell and Treiterer, 1968; Brackstone and McDonald, 1999], safety distance [e.g., Kometani and Sasaki, 1959; Gipps, 1981], action point [e.g., Michaels and Cozan, 1963; Evans and Rothery, 1977], and fuzzy logic based [e.g., Lan, et al. 1994; Chakroborty and Kikuchi, 1999; Wei and Lin, 1999; Lan and Yeh, 2001]. Among these four categories, stimulus-response type is the most famous one that was developed in the 1950s and 1960s by the General Motors (GM) research group. Five generations of the GM car-following models are recognized and nowadays they are still applied in various aspects, including traffic stability and safety study, level of service and capacity analysis, driver's reaction times, etc. However, Lan and Chang [2004b] constructed motorcycle-following models of General Motors and adaptive neuro-fuzzy inference system (ANFIS) and found that ANFIS was far superior to GM models in capturing the nature of motorcycle-following behaviors in a mixed traffic.

Recently, different cellular automata (CA) models have been developed to simulate the microscopic traffic flows according to some designated parallel updating rules. For instance, Krug and Spohn [1988] derived a simultaneous moving model for particles with maximum speed defaulted as 1 m/sec. This model is also called CA-184 rule because it corresponds to rule 184 in Wolfram's classification [Wolfram, 1986]. If the CA model controls only one particle's movement in random at each time step, it is called asymmetric stochastic exclusion process (ASEP). The NaSch model, proposed by Nagel and Schreckenberg [1992], combined the behaviors of ASEP and CA-184. Nagel [1996, 1998]

employed the concept of stochastic traffic cellular automata (STCA) and treated each particle with randomized integer speed between zero and maximum speed. Rickert et al. [1996] examined a simple two-lane CA model and pointed out important parameters defining the shape of the traffic fundamental diagram. Chowdhury et al. [1997] generalized the NaSch model by introducing a particle hopping model for two-lane traffic with two speed types (fast and slow) of vehicles. Nagel et al. [1998] proposed different CA approaches for the vehicle lane changing. Hermann and Kerner [1998] applied CA technique and self-organization process to explore the formation of traffic congestion. Knospe et al. [1999] dealt with the effect of slow cars in two-lane systems and found that even few slow cars could initiate the formation of platoons at low densities. Wolf [1999] employed a modified NaSch model to address the meta-stable states at the jamming transition in detail. Wang et al. [2000] introduced NaSch model and Fukui-Ishibashi (FI) model to investigate the asymptotic self-organization phenomena of one-dimensional traffic flow. Helbing [2001] considered the empirical data and then reviewed the main approaches including microscopic (particle-based), mesoscopic (gas-kinetic) and macroscopic (fluid-dynamic) models to modeling pedestrian and vehicle traffic. Further attention was also paid to the formulation of a micro-macro link, to aspects of universality and to other unifying concepts. Pottmeier et al. [2002] studied the impact of localized defect in a CA model for traffic flow exhibiting meta-stable states and phase separation. More recently, Bham and Benekohal [2004] developed a traffic simulation model based on CA and car-following concepts, which had been satisfactorily validated at the macroscopic and microscopic levels using two sets of field data.

Both the aforementioned conventional traffic flow models and recent CA traffic models are developed only for cars. None of them have been devoted to mixed traffic flows with motorcycles and cars. Unlike cars that normally move along a specific longitudinal lane and occasionally change lanes while overtaking or turning, motorcycles do not necessarily move within a specified lane. One can easily find that motorcycles in effect move in a rather irregular manner. Sometimes they may follow the lead vehicles; but more than often they just shift into the adjacent lanes erratically or even "sneak in" between two adjacent neighboring cars where no lane is marked. In other words, conventional traffic flow models and recent CA traffic models may not correctly elucidate such motorcycle moving behaviors, nor can they accurately reflect the true characteristics of mixed traffic in which motorcycles are involved. In many Asian countries such as China, Indonesia, Malaysia, Taiwan, Thailand and Vietnam, motorcycles are ubiquitous and mixed traffic flows with motorcycles and cars are also prevailing, particularly in the

urban areas. For the purpose of transportation system planning, design and control, it is always important to gain deep insights into the motorcycle behaviors by developing appropriate traffic flow models that can represent the vehicle movements in mixed traffic contexts.

This paper attempts to develop inhomogeneous CA models to describe the behaviors of vehicular movements in a mixed traffic environment. By inhomogeneous, we mean that different types of vehicles (car and motorcycle) occupy non-identical numbers of cell units, according to their required spaces for movements. Deterministic CA rules, based on the field observation, are proposed to govern the instantaneous positions and speeds of all particles. The CA models are validated by another set of field observed data. To account for the deviations of maximum speeds among individual particles, we further develop stochastic CA rules to analyze the mixed traffic characteristics with different traffic mixtures and roadway widths. The remaining parts are organized as follows. Section 2 details the development of deterministic CA rules and Section 3 presents the simulation results. Section 4 demonstrates the validation of results. Section 5 further introduces the stochastic CA rules by considering the deviations of maximum speeds among particles. Finally, the conclusions and directions of future study are addressed.

2. Models

To develop the inhomogeneous CA models, we need to define the dimensions of particles and cells and the rules of particle moving to comply with the real situations. A field survey was conducted on the southbound section of Tunhua South Road between Padeh Road and Civil Boulevard in Taipei City. The observed road section is a divided slow traffic lane of ten-meter width, traffic flow on which contains only two vehicle types, car and motorcycle, without any interrupted sink or source traffic from alleyways; curb parking is also prohibited. We used a video camera to record the traffic scenes, covering a longitudinal distance over 30 meters, during 8:00-9:30am and 16:00-17:30pm. The videotape was imposed with a synchronal timer so that the details of vehicular data could be measured to 0.01 second. The two-dimensional X- and Y-coordinates of all vehicles, i.e., the particles' longitudinal and lateral positions over time, were traced at least 30 meters so that the related characteristics including gaps, speeds, accelerations and decelerations could be calculated. It was found that the minimum gaps for a moving motorcycle and car were, respectively, 0.8 and 1.9 meters to the lead vehicle, 0.45 and 0.95 meters to the left neighboring vehicle,

and 0.4 and 0.82 meters to the right neighboring vehicle. The majority of the vehicles' maximum speeds were less than 55 kph with acceleration (deceleration) less than 1 meter/sec^2 during these two observation periods.

2.1 Definition of cells and particle sizes

A cellular automaton has a number of identical cells, each interacting with a few nearby neighbors by simple rules. The rules can be deterministic and/or stochastic. Each cell is in one of a small number of discrete states. Time advances in discrete steps and the cell states are updated either synchronously or asynchronously [Wolfram, 1986]. Previous CA traffic models [for instance, Nagel, 1998] defined the cell unit as 7.5×7.5 meters and assumed that each particle had identical size occupying one cell unit; namely, the space required for each vehicle was 7.5 meters both in length and in width. Because the definition of cell unit is too coarse, vehicles are modeled as particles with unrealistic speed jumps. This is obviously not the case what we have observed for the mixed traffic with cars and motorcycles.

In line with the vehicle dimensions and observed minimum gaps, we define a common cell unit with much finer square grid as 1.25×1.25 meters. Thus, based on the field observation, a motorcycle in our CA models occupies 2×1 cells and a passenger car takes away 6×2 cells while moving. In addition, we consider both "car-following" and "lane-changing" behaviors for each particle that changes its positions over time and over a two-dimensional space, in which X-axis indicates the vehicle's longitudinal movement distance and Y-axis denotes the vehicle's lateral displacement distance. Each cell can be either empty or occupied at each time step. The time step in updating the related information for all particles is set as one second so that the magnitude of speed (meters per second) is exactly equal to the longitudinal position change (meters). According to the filed survey, the maximum speeds for motorcycle and car are nearly the same, thus we set both with identical maximum speed as 13 cells (about 58kph). The gaps between the following particle (either motorcycle or car) and the front, right-front, left-front, right-behind and left-behind particles, respectively denoted by dX_f, dX_r, dX_l, dX_{rb}, and dX_{lb} are illustrated in Figure 1. In Figure 1(a), the i^{th} following particle is a motorcycle, which uses the 3^{rd} lateral cell lane with two motorcycles and two cars in both adjacent lanes. In Figure 1(b), the i^{th} following particle is a car, which occupies the 2^{nd} and 3^{rd} lateral cells with the same surrounding traffic situation. Note from Figures 1(a) and 1(b) that, even with exactly the same surrounding situation, the above-mentioned gaps are different because of the non-identical sizes of

the following particles.

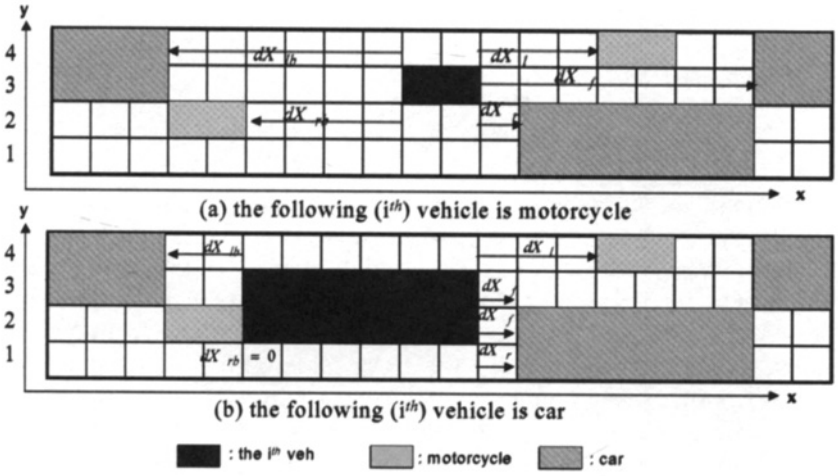

Figure 1. An illustration of inhomogeneous particles layout

2.2 Definition of CA rules

Nagel and Schreckenberg [1992] first introduced a prototype CA traffic model, which simulated single-lane (one-dimensional) pure car motions with simple updating rules. In the NaSch model, the road was divided into identical square cells of length 7.5 meters and each cell could either be empty or occupied by one car. The states of all cars at time step $t+1$ were obtained from those at time step t by applying the given rules at the same time. In this paper, we modify the NaSch model to simulate the two-dimensional mixed traffic motions with two different types of particles. We define the CA rules that govern the particles moving logics, including moving forward and lateral displacements from left to right or the reverse. Following the previous CA lane-changing models [Rickert et al. 1996; Chowdhury et al. 1997; Nagel et al. 1998; Knospe et al. 1999], we define a particle can change its "lane" (1.25-m cell in our definition) if both of the following two criteria are satisfied.

The first one is the incentive criterion: the gap in front of particle i at the current lane should be smaller than the current speed of i and the gap in front of i in the adjacent lane(s) should be larger than the current front gap of i. The second one is the safety criterion: any lateral displacement should not collide or block other vehicles behind. Thus, "lane changing"

is possible for vehicle i only when its adjacent lane(s) is empty and the speed of the left- or right-behind vehicle is smaller than the gap between vehicle i and the behind vehicle(s). Namely, the front gap of i in the adjacent lane(s) is larger than the current speed of i; and the behind gap of i in the adjacent lane(s) is larger than the current speed of behind vehicle. In fact, the above "lane changing" rules have included both symmetric and asymmetric situations. The particle that uses the intermediate cell(s) can make a symmetric lane change from both sides depending on which side provides larger gap. However, the particle that uses the edge (right-most or left-most) cell can only make an asymmetric lane change from one side in case that the adjacent gap is large enough.

Let dX^t_f, dX^t_l, dX^t_r, dX^t_b, dX^t_{lb} and dX^t_{rb} respectively denote the gaps between vehicle i and the front, left-front, right-front, behind, left-behind and right-behind vehicles at time step t; $\mathbf{P}^t_i = (x^t_i, y^t_i)$, $\mathbf{P}^t_f = (x^t_f, y^t_f)$, $\mathbf{P}^t_l = (x^t_l, y^t_l)$, $\mathbf{P}^t_r = (x^t_r, y^t_r)$, $\mathbf{P}^t_b = (x^t_b, y^t_b)$, $\mathbf{P}^t_{lb} = (x^t_{lb}, y^t_{lb})$ and $\mathbf{P}^t_{rb} = (x^t_{rb}, y^t_{rb})$ respectively denote the positions of vehicle i, front, left-front, right-front, behind, left-behind and right-behind vehicles at time step t. A random generator is used to determine the vehicles' initial positions. Let, $\mathbf{V}^t_i = (x^t_i, 0)$, $\mathbf{V}^t_l = (x^t_l, 0)$, $\mathbf{V}^t_r = (x^t_r, 0)$, $\mathbf{V}^t_b = (x^t_b, 0)$, $\mathbf{V}^t_{lb} = (x^t_{lb}, 0)$, and $\mathbf{V}^t_{rb} = (x^t_{rl}, 0)$ respectively denote the speed vectors of vehicle i, left-front, right-front, behind, left-behind and right-behind vehicles at time step t; L_i, L^t_f, L^t_l, and L^t_r denote the lengths of vehicle i, front, left-front and right-front vehicles at time step t; **PC** denote the vector of lateral position changed, in which **PC** = (0,-1) represents vehicle i changing to the right and **PC** = (0,1) changing to the left. Starting from an arbitrary initial condition with speed $\mathbf{V}^o_i = (v^o_i, 0)$ and $\mathbf{P}^o_i = (x^o_i, y^o_i)$ and position, the states of the particles in our CA models are updated according to the following rules:

(1) Estimate the desired speed $V_{desired}$ and the effective gaps dX^t_f, dX^t_l, dX^t_r, dX^t_b, dX^t_{lb} and dX^t_{rb};
(2) Check both incentive and safety criteria;
(3) Select the largest gap;
(4) Update the speeds;

Particle i updates its speed under the following logics:

If $dX^t_f > v^t_i$,

then $\mathbf{V}^{t+1}_i = Min\left[\mathbf{V}^t_i + (1,0), (v_{\max}, 0)\right]$;

Else, if $dX^t_l > v^t_i$ and $dX^t_{lb} > v^t_{lb}$ or $dX^t_r > v^t_i$ and $dX^t_{rb} > v^t_{rb}$

then change to larger-gap lane, $\mathbf{V}^{t+1}_i = \mathbf{V}^t_i + \mathbf{PC}$;

Else, cannot change lateral position,

$$\mathbf{V}_i^{t+1} = (v_i^{t+1},\ 0)$$

(5) Update the positions;
Particle i moves from P_t^i to P_i^{t+1} based on the updated speed; namely,

$$\mathbf{P}_i^{t+1} = \mathbf{P}_i^t + \mathbf{V}_i^{t+1}$$

3. Simulations

The initial conditions in the following simulations are set as follows. A total of 150 inhomogeneous particles (cars and motorcycles) are generated according to given traffic mixtures (percentages of car) from 0% to 100%. In the longitudinal direction, particles are equally spaced with distance headway (gap plus length of front particle) of 10 cells; however, in the lateral direction, particles are randomly scattered. Each particle moves at identical speed of 1 cell per second.

The aforementioned CA rules for updating the particle speeds and positions are used to simulate the particles' movements in the road section without interruptions by curb parking, pedestrian crossing, traffic light, etc. This study attempts five cases with "lane" width of 2 cell units (2.5m), 3 cell units (3.75m), 4 cell units (5m), 5 cell units (6.25m) and 6 cell units (7.5m). In both cases I (2.5m) and II (3.75m), it is impossible for any car to move in parallel along with the other car, thus the car has no chance to overtake another car. In other three cases, the car may have chances to overtake another car provided that the empty cells in the adjacent space are good enough. In contrast, it is possible for a motorcycle to move in parallel along with the lateral motorcycle(s). Except for the case I, the motorcycle can also overtake the front car or move in parallel along with the car.

3.1 The effects of lane widths and traffic mixtures

In this paper, cell occupancy (p) is used as a proxy of density, which is defined as $p = N_o / N$, where N is the number of total cells in the study area and N_o is the number of occupied cells. The flow-occupancy and speed-occupancy diagrams for pure motorcycles and pure cars under various lane widths are displayed in Figures 2 and 3, respectively. We define critical occupancy (critical speed) as the cell occupancy (space-mean-speed) corresponding to the maximum flow rates. With parallel updates, the steady state is reached when the speed of each

particle is the same as the speed of the front vehicle. The average speed in steady state equals the number of empty cells divided by the number of particles; hence, the average speed is inversely proportional to the cell occupancy (a proxy of density). Therefore, as the occupancies are smaller than the critical occupancy, the flow rates increase along with the increase of occupancies. However, as the occupancies go beyond the critical occupancy, the flow rates decrease gradually. Both Figures 2 and 3 show that the critical occupancies for pure motorcycles are around 0.13 to 0.18 and for pure cars are around 0.22 to 0.32. The range of critical occupancies for pure cars has concurred with the findings by Nagel [1998]. Both Figures 2 and 3 also show that the jammed occupancies for pure motorcycles can reach 1.0 in the five cases but for pure cars are only about 0.7 with an exception that case I can also reach 1.0. These phenomena are due to the fact that there is lower chance for pure cars to overtake the other particles; as a consequence, the cells utilization efficiency is less than that for pure motorcycles.

Figure 4 shows the relationship between maximum flow rates and traffic mixtures under various lane widths. Note that the maximum flow rates have a sharp decline from zero to 50 percentages of cars and a mild decline from 50 to 100 percentages in case I, implying that 50 percentages of cars could be the least cell utilization efficiency in case I.

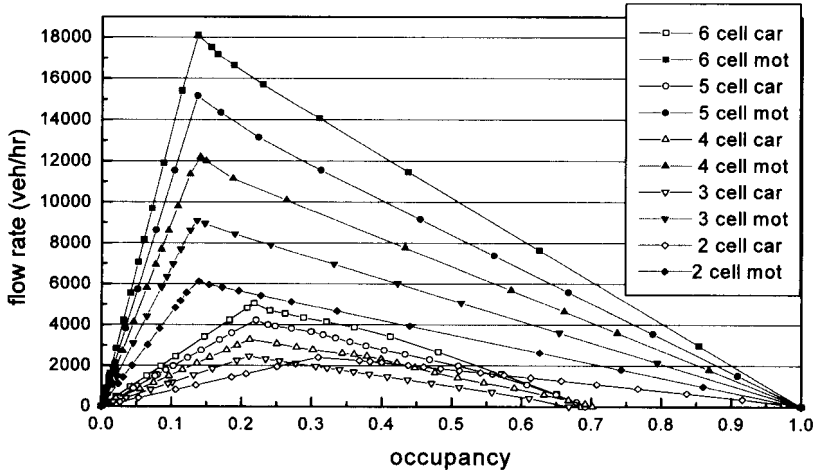

Figure 2. Flow-occupancy diagrams for pure motorcycles and pure cars

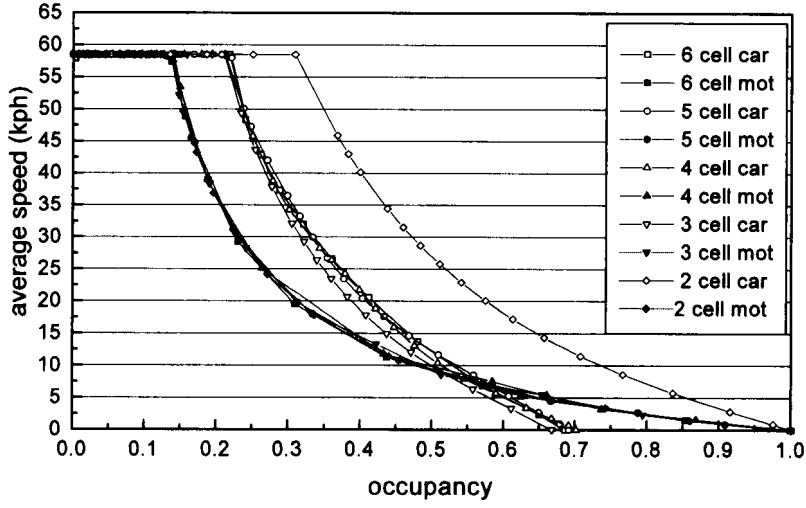

Figure 3. Speed-occupancy diagrams for pure motorcycles and pure cars

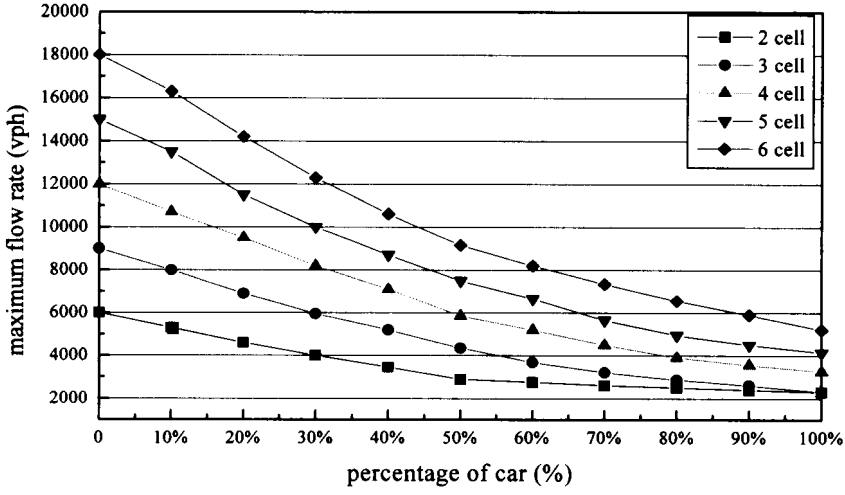

Figure 4. Maximum flow rates for various traffic mixtures

Furthermore, the maximum flow rates are highly influenced by the width of lane and percentages of car. For example, under the condition of pure motorcycles, the maximum flow rates in cases II and V are 50% and 200% higher than that in case I. Under the condition of pure cars, in contrast, the maximum flow rates are the same in both cases I and II, and case V is only 126% higher than both cases. The results also evidently explain that the following car cannot overtake the front car for both cases I and II.

3.3 The motorcycle equivalents (me)

Similar to the concept of "passenger car equivalent" (*pce*), which represents the throughput capability of one vehicle of other types (such as bus, truck) equivalent to the maximum number of car throughputs under identical traffic and environmental conditions, we define the "motorcycle equivalent" (*me*) as the throughput capability of one car equivalent to the maximum number of motorcycle throughputs under identical conditions. The value of me for any two traffic mixtures under the same speed condition is defined as follows:

$$me = \frac{q_1(1-P_1) - q_2(1-P_2)}{q_2P_2 - q_1P_1}$$

where P_1 , P_2 are the percentages of cars; q_1 , q_2 are the flow rates corresponding to P_1 and P_2. Note that the pce value is equal to 1/ *me*.

Table 1 summarizes the *me* and *pce* values under different traffic mixtures and lane widths. In case I, for example, the *me* values can range from 2.32 to 2.61 (at speed 55kph) and from 3.97 to 4.00 (at speed 5kph) with respect to 10% to 100% of cars. For pure cars with speed 55kph, the *me* values are from 2.61 to 3.46 as the lane width increases from two to six cells.

Figure 5 demonstrates the *me* values with respect to various speeds for pure cars. Note that the *me* values decrease as the speed increases in all cases. When cars get closer the average speeds would become lower; consequently, the *me* values should be higher. The lower *me* values occur in higher speeds, in which the efficiencies of cell utilization for cars and for motorcycles are nearer. Generally, the *me* values decrease as the lane width increases, indicating that wider roads provide higher degrees of freedom for particles' moving and overtaking than the narrower ones do.

Figure 6 illustrates the *me* values with respect to different percentages of car at speed 45 kph. We notice that case I has special *me*

values with respect to various car mixtures. It has the highest *me* values, the worst cells utilization efficiency, as the car percentages are lower than 50%. Nevertheless, it turns out to be the lowest *me* values, the best cells utilization efficiency, as the car percentages are above 60%. This interesting result reflects the fact that if motorcycles are the majority, once the cars appear, the following motorcycles would have no chance at all to overtake the cars in case I but the overtaking chance becomes higher as the lane width gets larger. In contrast, if cars become the majority in case I, the motorcycles will be grouped into several blocks by any two cars, thus makes the cell utilization better than the other cases.

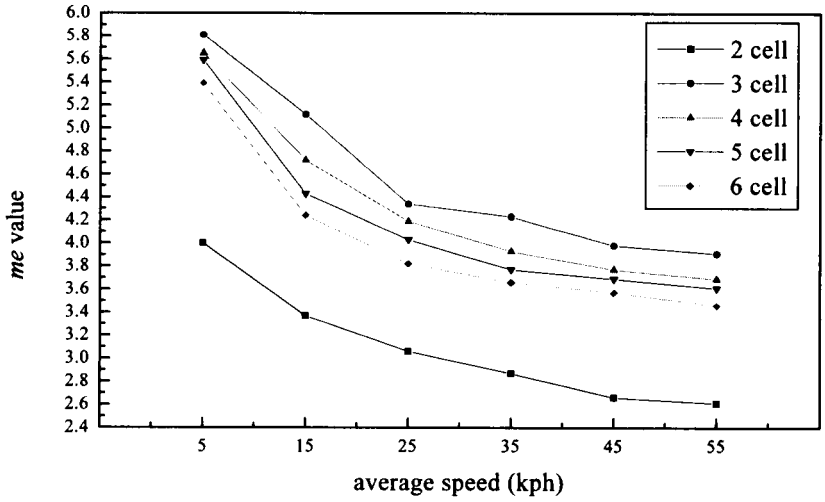

Figure 5. The *me* values at various speeds under pure cars

Table 1. The *me* and *pce* values under various traffic mixtures and lane widths

Speed	Percentage of cars	Case I 2 cells		Case II 3 cells		Case III 4 cells		Case IV 5 cells		Case V 6 cells	
(kph)	(%)	*me*	*pce*	*me*	*pce*	*me*	*pce*	*me*	*pce*	*me*	*pce*
	10	2.32	0.43	2.25	0.44	2.21	0.45	2.11	0.47	2.04	0.49
	20	2.52	0.40	2.47	0.40	2.32	0.43	2.25	0.44	2.21	0.45
	30	2.79	0.36	2.71	0.37	2.54	0.39	2.43	0.41	2.39	0.42
	40	2.91	0.34	2.83	0.35	2.73	0.37	2.71	0.37	2.67	0.38
55	50	3.17	0.32	3.14	0.32	3.10	0.32	3.00	0.33	2.93	0.34
	60	2.97	0.34	3.41	0.29	3.18	0.31	3.09	0.32	2.99	0.33
	70	2.87	0.35	3.59	0.28	3.38	0.30	3.30	0.30	3.07	0.33
	80	2.75	0.36	3.70	0.27	3.60	0.28	3.54	0.28	3.19	0.31
	90	2.67	0.38	3.74	0.27	3.64	0.27	3.59	0.28	3.28	0.30
	100	2.61	0.38	3.91	0.26	3.69	0.27	3.61	0.28	3.46	0.29
	10	2.52	0.40	2.44	0.41	2.33	0.43	2.25	0.44	2.17	0.46
	20	2.80	0.36	2.69	0.37	2.61	0.38	2.55	0.39	2.40	0.42
	30	2.94	0.34	2.83	0.35	2.71	0.37	2.59	0.39	2.51	0.40
	40	3.07	0.33	2.96	0.34	2.84	0.35	2.79	0.36	2.70	0.37
45	50	3.25	0.31	3.22	0.31	3.11	0.32	3.03	0.33	2.94	0.34
	60	3.01	0.33	3.50	0.29	3.29	0.30	3.20	0.31	3.02	0.33
	70	2.91	0.34	3.54	0.28	3.48	0.29	3.40	0.29	3.15	0.32
	80	2.80	0.36	3.68	0.27	3.61	0.28	3.50	0.29	3.21	0.31
	90	2.71	0.37	3.82	0.26	3.70	0.27	3.57	0.28	3.39	0.30
	100	2.66	0.38	3.98	0.25	3.77	0.27	3.69	0.27	3.57	0.28
	10	2.91	0.34	2.79	0.36	2.68	0.37	2.60	0.38	2.40	0.42
	20	2.75	0.36	2.82	0.35	2.79	0.36	2.77	0.36	2.74	0.37
	30	3.00	0.33	2.90	0.34	2.88	0.35	2.92	0.34	2.91	0.34
	40	3.09	0.32	3.03	0.33	2.93	0.34	2.94	0.34	2.94	0.34
35	50	3.57	0.28	3.49	0.29	3.32	0.30	3.16	0.32	3.16	0.32
	60	3.30	0.30	3.70	0.27	3.33	0.30	3.29	0.30	3.26	0.31
	70	3.13	0.32	3.71	0.27	3.69	0.27	3.64	0.27	3.33	0.30
	80	2.93	0.34	3.79	0.26	3.78	0.26	3.65	0.27	3.33	0.30
	90	2.85	0.35	3.96	0.25	3.82	0.26	3.71	0.27	3.46	0.29
	100	2.87	0.35	4.23	0.24	3.93	0.25	3.77	0.26	3.66	0.27
	10	3.30	0.30	3.16	0.32	3.04	0.33	2.83	0.35	2.60	0.38
	20	3.64	0.27	3.22	0.31	3.18	0.31	3.15	0.32	2.97	0.34
	30	3.82	0.26	3.30	0.30	3.25	0.31	3.21	0.31	3.19	0.31
	40	3.45	0.29	3.37	0.30	3.33	0.30	3.30	0.30	3.21	0.31
25	50	3.86	0.26	3.54	0.28	3.52	0.28	3.39	0.29	3.23	0.31
	60	3.58	0.28	3.86	0.26	3.57	0.28	3.43	0.29	3.33	0.30
	70	3.39	0.29	3.91	0.26	3.86	0.26	3.71	0.27	3.34	0.30
	80	3.36	0.30	3.97	0.25	3.94	0.25	3.74	0.27	3.53	0.28
	90	3.10	0.32	4.11	0.24	4.10	0.24	3.97	0.25	3.68	0.27
	100	3.06	0.33	4.34	0.23	4.19	0.24	4.03	0.25	3.82	0.26

Table 1 (continued). The *me* and *pce* values under various traffic mixtures and lane widths

Speed	Percentage of Cars	Case I 2 cells		Case II 3 cells		Case III 4 cells		Case IV 5 cells		Case V 6 cells	
(kph)	*(%)*	*me*	*pce*	*me*	*pce*	*me*	*pce*	*me*	*pce*	*me*	*pce*
	10	3.50	0.29	3.43	0.29	3.23	0.28	3.09	0.32	2.79	0.36
	20	3.81	0.26	3.80	0.26	3.59	0.28	3.32	0.30	3.27	0.31
	30	4.01	0.25	3.94	0.25	3.70	0.27	3.35	0.30	3.30	0.30
	40	4.26	0.23	3.41	0.29	3.81	0.26	3.36	0.30	3.31	0.30
15	50	4.30	0.23	4.21	0.24	4.15	0.24	3.62	0.28	3.46	0.29
	60	3.89	0.26	4.29	0.23	4.22	0.24	3.96	0.25	3.72	0.27
	70	3.74	0.27	4.80	0.21	4.43	0.23	4.07	0.25	3.93	0.25
	80	3.66	0.27	4.91	0.20	4.49	0.22	4.23	0.24	4.03	0.25
	90	3.49	0.29	4.97	0.20	4.61	0.22	4.25	0.24	4.10	0.24
	100	3.37	0.30	5.12	0.20	4.72	0.21	4.43	0.23	4.24	0.24
	10	3.97	0.25	3.86	0.26	3.63	0.28	3.42	0.29	3.18	0.31
	20	4.28	0.23	4.00	0.25	3.74	0.27	3.41	0.29	3.26	0.31
	30	4.33	0.23	4.15	0.24	4.07	0.25	3.52	0.28	3.45	0.29
	40	4.50	0.22	4.31	0.23	4.21	0.24	3.89	0.26	3.74	0.27
5	50	4.65	0.22	4.54	0.22	4.33	0.23	4.13	0.24	3.87	0.26
	60	4.67	0.21	5.05	0.20	4.49	0.22	4.21	0.24	4.17	0.24
	70	4.47	0.22	5.42	0.18	4.85	0.21	4.74	0.21	4.47	0.22
	80	4.37	0.23	5.52	0.18	5.11	0.20	4.88	0.21	4.72	0.21
	90	4.19	0.24	5.60	0.18	5.50	0.18	5.36	0.19	4.97	0.20
	100	4.00	0.25	5.81	0.17	5.65	0.18	5.59	0.18	5.39	0.19

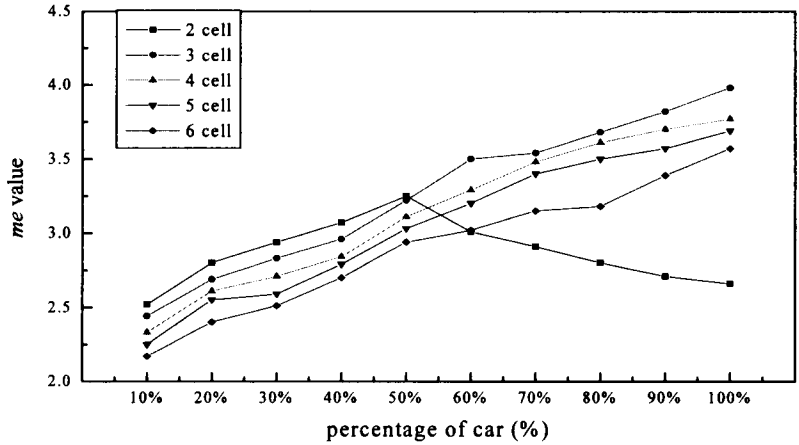

Figure 6. The *me* values for various traffic mixtures at speed 45 kph

4. Validation

In order to validate the proposed inhomogeneous CA models, we conducted a two-hour survey (16:30 to 18:30pm) in the T-2 Provincial Highway at Chuwei of Taipei County. The southbound mixed traffic scenes in the outer lane of 3.5-meter width were recorded by a video camera and a total of 4,882 vehicles were observed (motorcycles are prohibited in the inner lanes). This survey has obtained 120 one-minute flow rates with corresponding speeds and densities. Figure 7 displays the speed-flow relationship for these 120 samples. Figure 8 further shows the space mean speed distributions for individual motorcycles and cars, which approximately follow normal distributions with mean 55 kph and standard deviation 11.8 kph.

Note from Figure 8 that the speeds for motorcycles in the T-2 Highway are slightly higher than the cars. Thus, we further undertake a statistical test and the result ($X^2 - 81.71 > X^2_{(0.05,10)} = 18.3$) has rejected the null hypothesis that speed is independent of the vehicle type. Therefore, we modify the aforementioned CA parameters by assigning the car with maximum speeds of 12 cell units (54 kph) and the motorcycle with 13 cell units (58.5 kph). The field observed data in T-2 Highway and the simulated data are presented in Figure 9 and Table 3. Note that most of the discrepancies between the observed and simulated data are less than ± 5%, suggesting that our CA rules have been validated by another field observation.

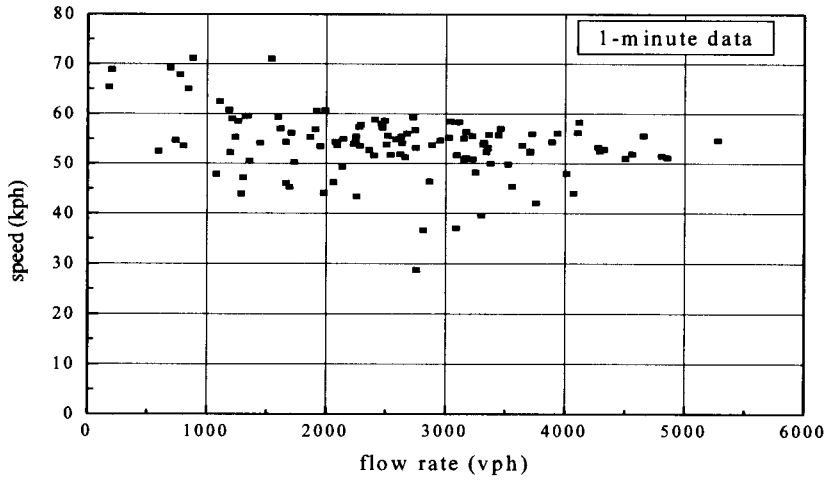

Figure 7. Observed space mean speeds versus flow rates in T-2 Highway

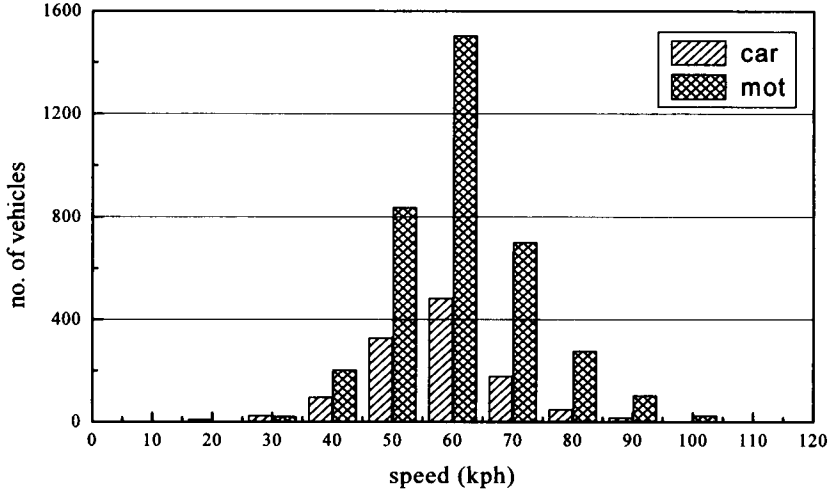

Figure 8. Observed space mean speed distributions in T-2 Highway

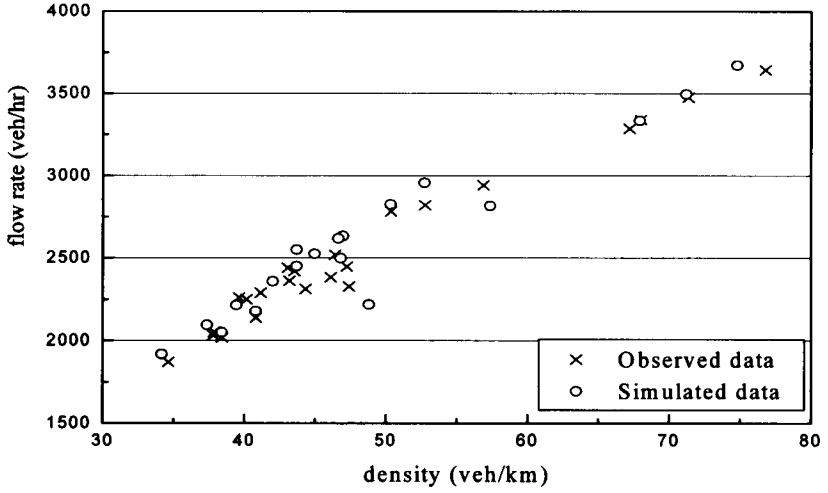

Figure 9. Observed and simulated flow-density in T-2 Highway

Table 2. A comparison between observed and simulated data in T-2 Highway

Observed percentages of motorcycle	Observed data*			Simulated data**			Flow rate (%)
	Speed (kph)	Flow rate (vph)	Density (vpk)	Speed (kph)	Flow rate (vph)	Density (vpk)	
61%	52.54	2,018	38.42	53.38	2,050	38.40	1.56%
61%	52.38	2,138	40.82	53.38	2,178	40.80	1.87%
78%	54.00	1,870	34.63	56.16	1,918	34.16	2.59%
66%	51.82	2,447	47.23	56.09	2,634	46.96	7.63%
63%	51.69	2,383	46.10	53.38	2,498	46.80	4.83%
71%	54.69	2,362	43.18	56.09	2,450	43.68	3.73%
70%	53.73	2,032	37.81	56.09	2,095	37.36	3.12%
67%	48.89	3,286	67.21	49.10	3,335	67.92	1.49%
81%	47.45	3,644	76.80	49.10	3,673	74.80	0.77%
77%	49.12	3,341	68.01	49.10	3,335	67.92	-0.18%
72%	48.68	3,475	71.37	49.10	3,496	71.20	0.61%
71%	53.48	2,821	52.76	56.09	2,957	52.72	4.80%
81%	55.25	2,782	50.35	56.16	2,826	50.32	1.59%
72%	51.73	2,942	56.87	49.10	2,816	57.36	-4.27%
83%	52.19	2,313	44.32	56.16	2,525	44.96	9.15%
73%	56.66	2,440	43.06	56.09	2,450	43.68	0.42%
79%	55.65	2,290	41.15	56.16	2,359	42.00	3.00%
76%	54.27	2,518	46.40	56.16	2,619	46.64	4.00%
78%	56.08	2,251	40.14	56.16	2,359	42.00	4.78%
91%	55.63	2,421	43.53	58.39	2,550	43.68	5.33%
80%	57.07	2,261	39.62	56.16	2,215	39.44	-2.05%
72%	54.20	2,053	37.87	56.09	2,095	37.36	2.08%
74%	49.13	2,328	47.39	45.48	2,219	48.80	-4.68%

Note: *speed and flow rate are measured from the observed data; density are calculated from dividing flow rate by speed.
**speed and density are measured from the simulated data; flow rate are calculated from the product of speed and density.

5. Stochastic CA models

One of our deterministic CA rules has set the maximum speeds for individual vehicles of the same type with a fixed value. Of course, this assumption is too strict and does not fully fit the real world situations. Therefore, we further allow the deviations of maximum speeds for individual particles by modifying the CA rules with stochastic maximum speed distributions. Take an example that the maximum speeds are normally distributed with mean 13 cells and standard deviation 1 cell, denoted by $N(13,1)$. The flow-occupancy and speed-occupancy diagrams for pure cars and pure motorcycles with stochastic maximum speeds $N(13,1)$ are shown in Figures 12 and 13. Compared with Figures 2 and 3 obtained from deterministic maximum speeds $N(13,0)$, we find that both maximum flow rates and critical speeds by the stochastic CA models have decreased. It is due to the "slow-vehicle" effects.

In this $N(13,1)$ example, Figure 12 further presents the maximum flow rates with respect to various traffic mixtures. Figure 13 displays the *me* values for various maximum speeds under pure car condition. Figure 14 shows the *me* values with respect to various traffic mixtures at speed 45 kph. Compared with Figures 6, 7 and 8 obtained from deterministic maximum speeds $N(13,0)$, we find that the corresponding *me* values for the stochastic CA models are apparently higher. It explains that with the variation of maximum speeds, some slow vehicles have reduced the overall particles moving freedom.

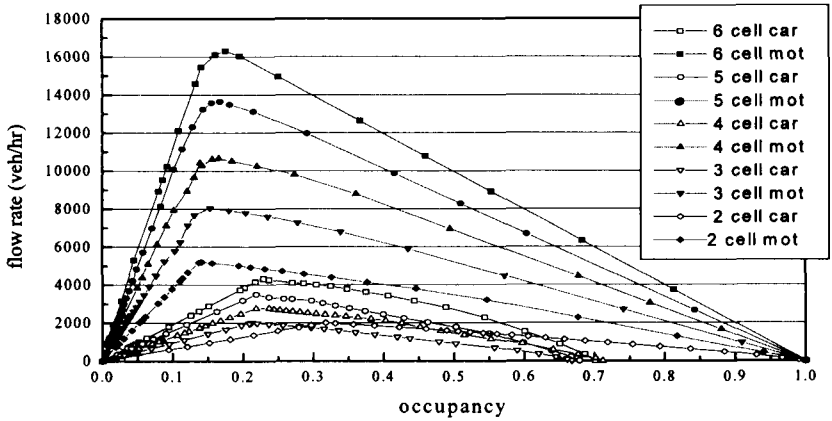

Figure 10. Flow-occupancy diagrams for pure motorcycles and pure cars (Stochastic CA models with maximum speeds ~ $N(13,1)$)

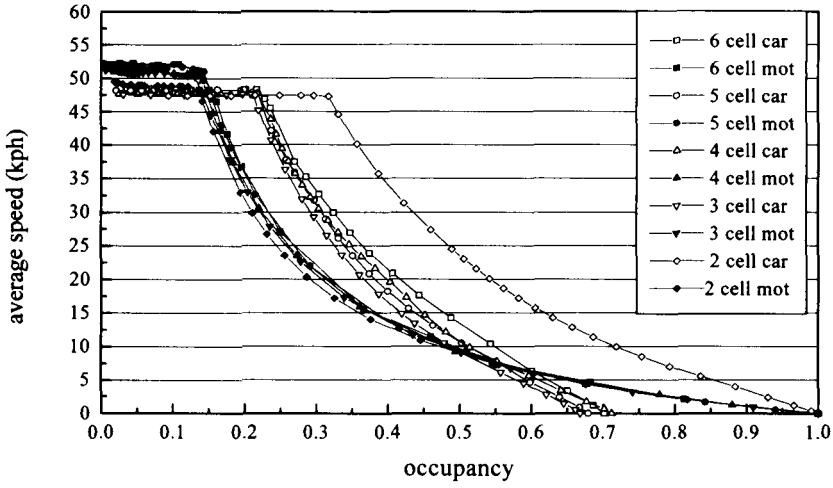

Figure 11. Speed-occupancy diagrams for pure motorcycles and pure cars
(Stochastic CA models with maximum speeds ~ $N(13,1)$)

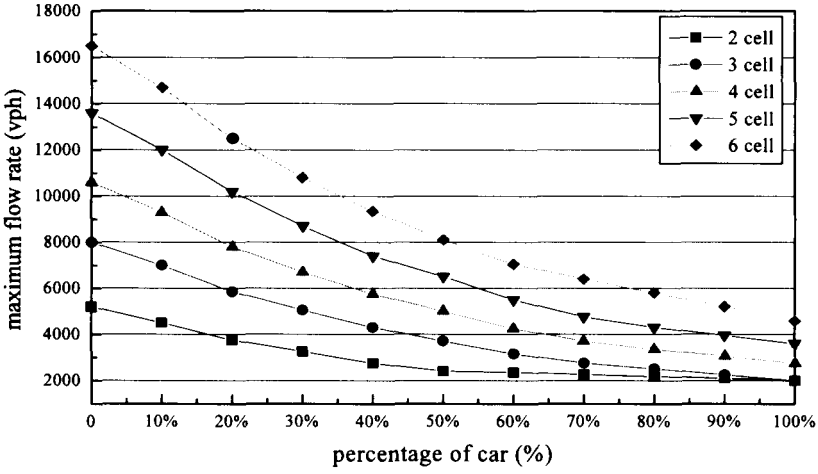

Figure 12. Maximum flow rates for various traffic mixtures
(Stochastic CA models with maximum speeds ~ $N(13,1)$)

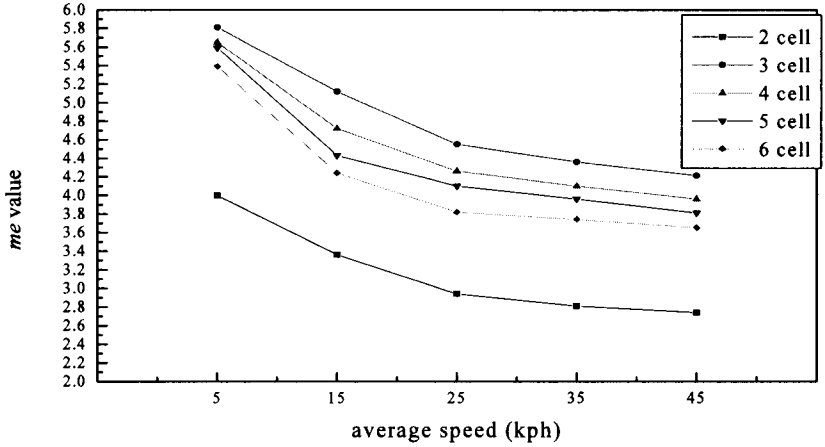

Figure 13. The *me* values at various speeds under pure car condition (Stochastic CA models with maximum speeds ~ N (13,1))

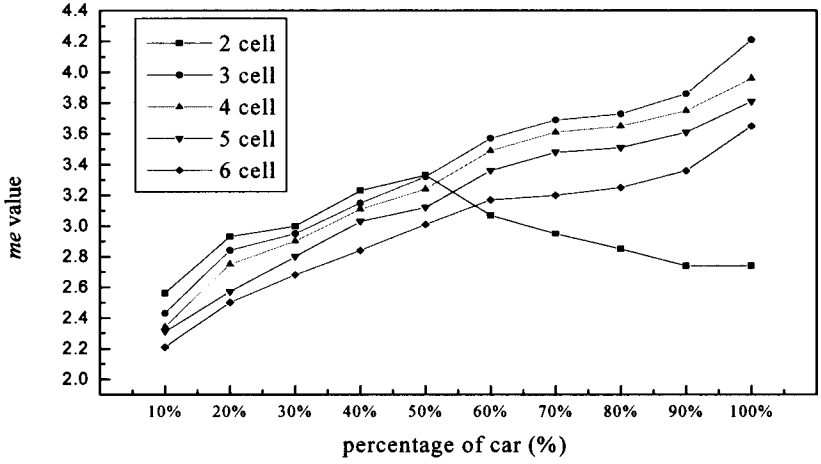

Figure 14. The *me* values for various traffic mixtures at speed 45 kph (Stochastic CA models with maximum speeds ~ N (13,1))

Figures 17 and 18 further compare the simulation results for pure motorcycles and pure cars among different standard deviations of maximum speeds (zero, one and two standard deviations): N (13,0), N (13,1) and N (13,2). We find that as the maximum speed deviations get larger, the optimal speeds and maximum flow rates have significantly declined. Tables 4 and 5 present the details of maximum flow rates and optimal speeds among different maximum speed deviations. We conclude that the maximum flow rates and critical speeds are negatively influenced by the deviation of maximum speeds; but the influence is less significant as the lane width gets larger.

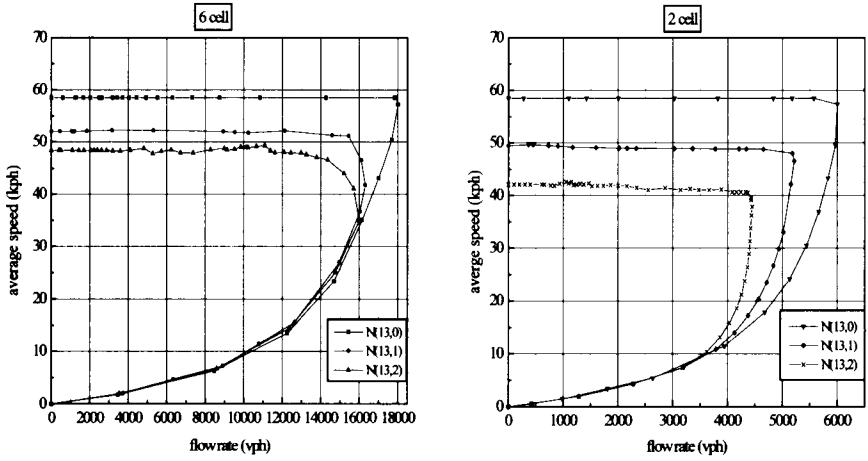

Figure 15. Speed-flow diagrams of CA models with various maximum speed deviations (pure motorcycles)

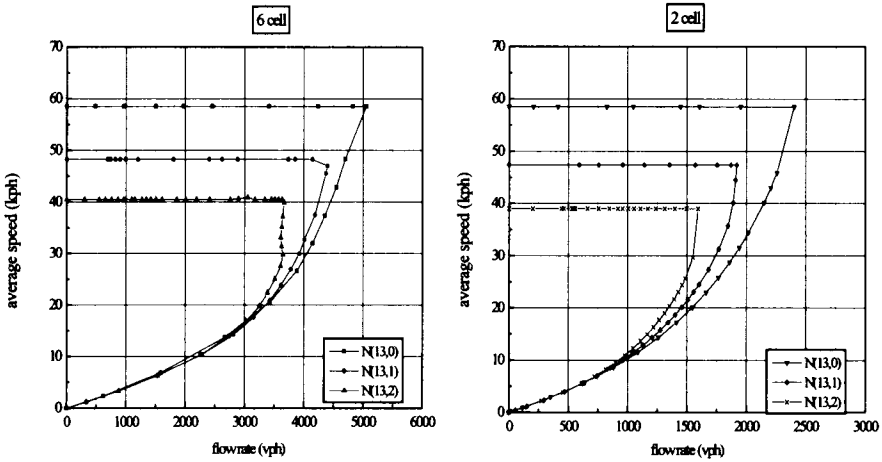

Figure 16. Speed-flow diagrams of CA models with various maximum speed deviations (pure cars)

Table 3. Maximum flow rates with various maximum speed deviations

Lane width	Pure motorcycles (vph)					Pure cars (vph)				
	N(13,0)	*N(13,1)*		*N(13,2)*		*N(13,0)*	*N(13,1)*		*N(13,2)*	
	a	b	(b-a)/a	c	(c-a)/a	d	e	(e-d)/d	f	(f-d)/d
2 cells (2.5 m)	6,000	5,200	-13.3%	4,450	-25.8%	2,300	1,900	-17.4%	1,550	-32.6%
3 cells (3.75 m)	9,000	8,000	-11.1%	7,200	-20.0%	2,300	1,900	-17.4%	1,550	-32.6%
4 cells (5 m)	12,000	10,680	-11.0%	9,800	-18.3%	3,250	2,700	-16.9%	2,250	-30.8%
5 cells (6.25 m)	15,000	13,400	-10.7%	12,800	-14.7%	4,150	3,520	-15.2%	2,900	-30.1%
6 cells (7.5 m)	18,000	16,250	-9.7%	15,950	-11.4%	5,200	4,450	-14.4%	3,650	-29.8%

Table 4. Critical speeds with various maximum speed deviations

Lane width	Pure motorcycles (kph)			Pure cars (kph)		
	N(13,0)	*N(13,1)*	*N(13,2)*	*N(13,0)*	*N(13,1)*	*N(13,2)*
2 cells (2.5 m)	58.5	49.5	42.0	58.5	47.5	39.0
3 cells (3.75 m)	58.5	51.0	44.6	58.5	47.5	39.0
4 cells (5 m)	58.5	51.3	47.0	58.5	47.7	39.3
5 cells (6.25 m)	58.5	51.8	47.1	58.5	48.2	40.0
6 cells (7.5 m)	58.5	52.0	48.4	58.5	48.3	40.5

6. Concluding Remarks

Previous works on CA traffic models focused on pure cars only. Some of which defined the cell unit with a rather coarse scale, thus the particles might have unrealistic speed jumps or drops. This is obviously not consistent with what we can observe in the mixed traffic contexts. To overcome these shortcomings, we define a common cell unit with much finer square grid as 1.25×1.25 meters. Based on the field observation, a motorcycle in our proposed CA models always occupies 2×1 cells and a passenger car always takes away 6×2 cells. The maximum speeds for the motorcycle and car are of the same, which are set as 13 cell units per time step with no deviation in our deterministic CA models. The simulation results have shown reasonable interacting relationships among particles in the mixed traffic environments. To validate the deterministic CA models, we use another set of field data where maximum speeds of motorcycle and car are not the same; thus, the CA rules have been slightly modified to accommodate the distinct maximum speeds between these two vehicle types.

In line with the real world situations, we further develop stochastic CA models by considering the deviations of maximum speeds for individual particles of the same type. Compared with the deterministic CA models, we examine the effects of maximum speed deviations on the maximum flow rates and the corresponding critical speeds. It is found that both maximum flow rates and critical speeds have declined with an increase of maximum speed deviations. It is due to the slow-vehicle effect that deteriorates the cell utilization efficiency; however, such decline effect is less significant as the road (lane) gets wider.

The present study does not mark the lane to guide the motorcyclists and car drivers, thus the vehicles may occupy the lateral cells in an inefficient manner. Marking the lanes and revising the CA rules accordingly deserve further investigation. The paper deals only with the interacting movements of two vehicle types, motorcycle and car, on the road section where flows are not interrupted by curb parking, crossing vehicles or pedestrians, traffic signals or the like. Future studies can consider more types of vehicles, such as bus and bicycle, with interruptions or traffic lights on the road section or at intersection. However, it requires introducing more complicated CA rules that can govern the particles stopping, starting, moving or turning behaviors. Special attentions must be paid to control the particles acceleration or deceleration to avoid any unrealistic abrupt speed jumps or drops. Since the motorcyclists and car drivers may act in a different way in other cities or countries, more empirical case studies from different field environments also deserve further explorations.

Acknowledgements

This paper is moderately revised from the original work [Lan and Chang, 2004a] presented at the International Conference on Application of Information and Communication Technology in Transport Systems in Developing Countries, Kalutara, Sri Lanka. The research was granted by the National Science Council of ROC (NSC93-2211-E-009-033). The authors are indebted to two reviewers for giving very good suggestions to ameliorate the original paper.

References

Bham, G. H. and Benekohal, R. F., 2004. A high fidelity traffic simulation model based on cellular automata and car-following concepts. Transportation Research 12C, 1-32.

Bierley, R. L., 1963. Investigation of an inter-vehicle spacing display. Highway Research Record 25, 58-75.

Brackstone, M. and McDonald, M., 1999. Car-following: a historical review. Transportation Research 2F, 181-196.

Chakroborty, P. and Kikuchi, S., 1999. Evaluation of the general motors based car-following models and a proposed fuzzy inference model. Transportation Research 7C, 209-235.

Chowdhury, D., Wolf, D. E. and Schreckenberg, M., 1997. Particle-hopping models for two-lane traffic with two kinds of vehicles: effects of lane-changing rules. Physica 235A, 417-439.

Daganzo, C. F., 1994. The cell transmission model: a dynamic representation of highway traffic consistent with the hydrodynamic theory. Transportation Research 28B, 269-287.

Daganzo, C. F., 2002a. A behavioral theory of multi-lane traffic flow. Part I: Long homogeneous freeway sections. Transportation Research 36B, 131-158.

Daganzo, C. F., 2002b. A behavioral theory of multi-lane traffic flow. Part II: Merges and the onset of congestion. Transportation Research 36B, 159-169.

Evans, L. and Rothery, R., 1977. Perceptual thresholds in car following - a recent comparison. Transportation Science 11, 60-72.

Gipps, P. G., 1981. A behavioral car following model for computer simulation. Transportation Research 15B, 105-111.

Helbing, D., 2001. Traffic and related self-driven many-particle systems. Reviews of Modern Physics 73, 1067-1141.

Herman, R., Montroll, E. W., Potts, R. B. and Rothery, R. W., 1959. Traffic dynamics: analysis of stability in car following. Operations Research 7, 86-106.

Hermann, M. and Kerner, B. S., 1998. Local cluster effect in different traffic flow models. Physica 255A, 163-188.

Knospe, W., Santen, L., Schadschneider, A. and Schreckenberg, M., 1999. Disorder effects in cellular automata for two-lane traffic. Physica 265A, 614-633.

Kometani, E. and Sasaki, T., 1959. A safety index for traffic with a linear spacing. Operations Research 7, 707-720.

Krug, J. and Spohn, H., 1988. Universality classes for deterministic surface growth. Physical Review 83A, 4271-4286.

Lan, L. W., Wang, J. C. and Chiang, C. I., 1994. On the car following model with fuzzy control. Transportation Quarterly 25, 43-55.

Lan, L. W. and Yeh, H. H., 2001. Car following behavior for drivers with non-identical risk aversion: ANFIS approach. Journal of the Chinese Institute of Civil & Hydraulic Engineering 13, 427-434.

Lan, L. W. and Chang, C. W., 2004a. Inhomogeneous particles hopping models for mixed traffic with motorcycles and cars. International Conference on Application of Information and Communication Technology in Transport Systems in Developing Countries, Kalutara, Sri Lanka, August 5-7.

Lan, L. W. and Chang, C. W., 2004b, Motorcycle-following models of

General Motors (GM) and adaptive neuro-fuzzy inference system (ANFIS). Transportation Planning Journal 33, 511-536.

Lighthill, M. H. and Whitham, G. B., 1955. On kinematic waves: a theory of traffic flow on long crowed roads. Proceedings of the Royal Society, Series A 229, 317-345.

Liu, G., Lyrintzis, A. S., and Michalopoulus, P. G., 1998. Improved high-order model for freeway traffic flow. Transportation Research Record 1644, 37-46.

May, A. D., 1990. Traffic Flow Fundamentals. Prentice-Hall Inc., New Jersey.

Michaels, R.M. and Cozan, L. W., 1963. Perceptual and field factors causing lateral displacement. Highway Research Record 25, 1-13.

Nagel, K. and Schreckenberg, M., 1992. A cellular automaton model for freeway traffic. Journal de Physique I France 2, 2221-2229.

Nagel, K., 1996. Particle-hopping models and traffic flow theory. Physical Review 53E, 4655-4672.

Nagel, K., 1998. From particle-hopping models to traffic flow theory. Transportation Research Record, 1644, 1-9.

Nagel, K., Wolf, D. E., Wagner, P. and Simon, P., 1998. Two-lane traffic rules for cellular automata: A systematic approach. Physical Review 58E, 1425-1437.

Payne, H. J., 1971. Model of freeway traffic and control. Mathematics of Public Systems 1, 51-61.

Pipes, L. A., 1967. Car following models and the fundamental diagram of road traffic. Transportation Research Record 1, 21-29.

Pottmeier, A., Barlovic, R., Knospe, W. and Schadschneider, A., 2002. Localized defects in a cellular automaton model for traffic flow with phase separation. Physica 308A, 471-482.

Richards, P. I., 1956. Shock waves on highway. Operations Research 4, 42-51.

Rickert, M., Nagel, K., Schreckenberg, M. and Latour, A., 1996. Two lane traffic simulation using cellular automata. Physica 231A, 534-550.

Rockwell, T. H. and Treiterer, J., 1968. Sensing and communication between vehicles. NCHRP Report 51, HRB, Washington, D.C.

Wang, B. H., Wang, L., Hui, P. M. and Hu, B., 2000. The asymptotic steady states of deterministic one-dimensioned traffic flow models. Physica 27B, 237-239.

Wei, C. H. and Lin, H. C., 1999. Construction of car-following models using artificial neural networks and genetic algorithms. Transportation Planning Journal 28, 353-378.

Wolf, D. E., 1999. Cellular automata for traffic simulations. Physica 263A, 438-451.

Wolfram, S., 1986. Theory and Applications of Cellular Automata. Word Scientific, Singapore.

Wong, G. C. K. and Wong, S. C., 2002. A multi-class traffic flow model – an extension of LWR model with heterogeneous drivers. Transportation Research 36A, 827-841.

Zhang, H. M., 1998. A theory of nonequilibrium traffic flow. Transportation Research 32B, 485-498.